encit 2020

ABCM
Associação Brasileira de Engenharia e Ciências Mecânicas

18th Brazilian Congress of Thermal Sciences and Engineering
November 16–20, 2020 (Online)

ENC-2020-0193
HYDROUS ETHANOL ATOMIZATION BY IMPINGING JETS

Gabriel Silva Dias
Danilo Almeida Machado
José Carlos de Andrade
Fernando de Souza Costa
Combustion and Propulsion Laboratory - LABCP
National Institute for Space Research - INPE
Rodovia Presidente Dutra, km 40, CEP 12.630-000
Cachoeira Paulista, São Paulo, Brazil
gabriel.dias@inpe.br

Abstract. *Liquid propellant engines are the most used configuration in rocket propulsion systems. Ethanol was extensively used as liquid fuel in rocket propulsion systems, it has the advantage of be safe to handle and a green propellant. Impinging injectors are widely used due their easy of manufacture and efficiency. This experimental work atomizes liquid hydrous ethanol using impinging jets. Shadow images were taken in order to analyze the free jet and the sheet formed under a range of jet velocities. The free jet flow in ambient air 6 mm downstream the exit was turbulent for $u > 5$ m/s and the registered regimes of formed liquid sheet went from closed stable sheet to impact wave. A brief analysis about coalescence and secondary droplet breakup was done based on literature simplified models. A Spraytec laser diffraction system was used to obtain representative diameters and droplet size distributions. Representative diameters presented no clear trend with jet Reynolds number, however it SMD and D_{v10} seemed to decrease with increase of impingement angle. Bimodal particle size distributions presented a detachment trend of the two droplet populations as the jet velocity increased, however the population of larger droplets tends to increase in volume frequency, such effect may be a result of both secondary atomization together with coalescence.*

Keywords: *Impinging jets, Atomization, Ethanol, Green propellant, Spray*

1. INTRODUCTION

Liquid propellant rocket engines have been used as the primary propulsion system for many launch vehicles since the late 1920s. The performance of a rocket engine is determined not only by the selection of propellants but also by performance of the atomization process provided by the injectors. Atomization is an essential process that occurs on the propulsion systems, it accelerates vaporization by breaking up the bulk fuel into droplets and distributes it throughout the combustion chamber. In atomization, the surface area of the liquid phase is increased until the process becomes unstable, leading to disintegration of the liquid interface into droplets. Small droplets are required to achieve rapid ignition and establish a flame front adjacent to the injection head. Large droplets take longer to burn and defines the combustion chamber length (Ghafourian *et al.*, 1991) (Khavkin, 2004). Atomization can be achieved by different injection methods such as dual orifice or coaxial jets, impinging jets, rotary and electrostatic (Ghafourian *et al.*, 1991).

Impinging jets have been extensively studied until nowadays (Deng *et al.*, 2018) (Negri and Ciezki, 2016)(Ramasubramanian *et al.*, 2015)(Connell *et al.*, 2018)(Chen and Yang, 2019). Impinging jets are used by their easy of manufacture and simultaneous good atomization and mixing to achieve an efficient mixing and burning of propellants. Two impinging jets with equal diameter D and velocity u impinges at a certain impingement angle 2θ to form a sheet in a plane perpendicular to that of the momentum vectors of the jets. Figure 1 shows a sheet formed by the collision of two identical jets (like impingement) of hydrous ethanol. When u is relatively low, the sheet is closed and a rim is visible. Waves form on the sheet and grow until the sheet fragmentation into ligaments, that later breaks up into drops (Fakhri *et al.*, 2010).

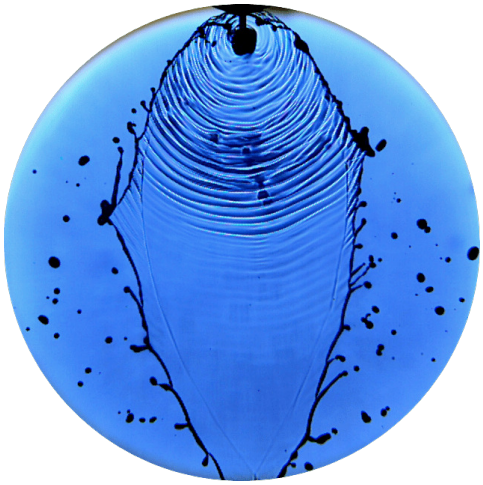

Figure 1. Hidrous ethanol liquid sheet, $2\theta = 90^o$, u = 3.5 m/s

Ethanol is a green propellant that was extensively used as rocket propellant worldwide, including the under development Brazilian Liquid Propellant Rocket Engine, L75.

Therefore this work aims to study the atomization behavior of hydrous ethanol using impinging jets. Shadow pictures of free jets in ambient air and of formed sheet at low jet velocities, representative diameters and droplet size distributions obtained with a laser diffraction system considering multi-modality are the scope of this experimental work.

2. METHODOLOGY AND MATERIALS

Dimensionless numbers have an important role in analyzing the behavior of fluids.

Reynolds number (*Re*) is the ratio of inertial and viscous forces, and is frequently used to determine whether the fluid flow is laminar or turbulent:

$$Re = \frac{\rho u D}{\mu} \tag{1}$$

where ρ is the fluid density, *D* is the orifice diameter, u is the jet velocity, *D* the exit orifice diameter, and μ the viscosity.

Weber number (*We*) is the ratio between inertia and surface tension forces, a dimensionless number often used when there is an interface between two different fluids:

$$We = \frac{\rho u^2 D}{\sigma} \tag{2}$$

where σ is the surface tension.

A spray is generally considered to be a droplet system immersed in a continuous gas phase. Due to the heterogeneous nature of the atomization process, the ligaments formed by the various disintegration mechanisms of jets and films vary the diameter of the drops and the corresponding average diameters. Injectors in practice do not produce uniform droplet size sprays under a given operating condition, but instead, the spray contains a droplet size spectrum distributed over some arbitrarily defined average values (Lefebvre, 1988).

In many problems is convenient to work only with mean diameters rather than the complete droplet size distribution. A generalized mean diameter can be defined as (Lefebvre, 1988):

$$D_{ab} = \left(\frac{\sum N_i D_i^a}{\sum N_i D_i^b} \right)^{1/(a-b)} \tag{3}$$

where *a* and *b* can have any values corresponding to the effect investigated and the sum *a*+*b* is called average diameter order, *i* denotes the range of droplet size considered, N_i is the number of droplets in the droplet size range *i* and D_i is the average diameter of the droplet size range of drops *i*.

For most engineering proposals, the droplet size distribution in a spray can be represented concisely as a function of two parameters, one of which is a representative mean diameter and the other a measure of the droplet size range. A representative diameter commonly used for combustion applications is the Sauter Mean diameter *SMD* or D_{32} (when in Equation 3 *a* = *3* and *b* = *2*), is used to describe the atomization performance. Others representative diameters widely used are Dv_{10}, Dv_{50} and Dv_{90}, where 10%, 50% or 90% of the total atomized volume consists of droplets with diameters less than or equal to the indicated value.

Figure 2. Schematic of different modes of secondary droplet breakup. (Ashgriz, 2011)

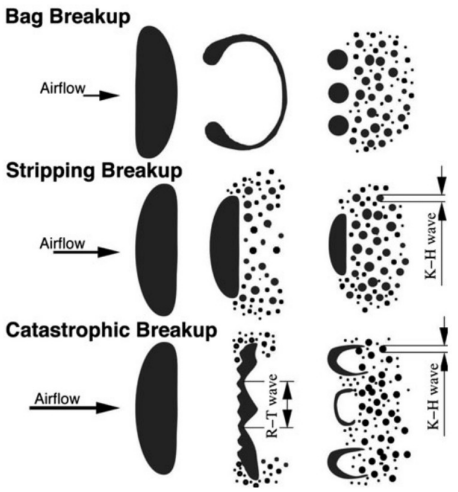

Droplets may suffer deformation and secondary atomization. A division according secondary atomization (Figure 2) based on experimental observations was reported and it seems to be dependent only on Weber number of the droplet (Faeth *et al.*, 1995).

According to Faeth *et al.* (1995), the Weber number ranges are approximately the following:

- 12 < *We* < 20, Bag breakup;
- 20 < *We* < 80, Multimode breakup;
- 80 < *We* < 800, Shear/stripping breakup;
- 800 < *We*, Catastrophic breakup.

where *We* in that case uses the ambient gas density, droplet velocity, the initial droplet diameter and the surface tension between the fluid and ambient gas (Equation 2).

Still according to Faeth *et al.* (1995) for high values of the liquid's viscosity the limits of breakup regimes are affected, as the viscosity increases, the value of *We* required for the onset of breakup increases.

Droplet collision is another relevant physical process for fluid dynamics that occurs, for example, in coating processes and motor fuel injection. Such phenomena may significantly modify the spray characteristic droplet sizes and velocities. Studying droplet interactions in a whole spray or between several impinging sprays is a very difficult task. In order to simplify this problem, many authors consider binary droplet collisions in a spray. Experimental results lead to the classification of five different outcome regimes: coalescence with minor deformation, bouncing, coalescence with large deformation, reflexive separation, and stretching separation. A criterion for coalescence based on experimental results was proposed as (Rabe *et al.*, 2010):

$$We_s \leq 0.45 \qquad and \qquad I < \frac{\sqrt{0.53^2 + 8(0.53We_s)} - 0.53}{4.We_s} \tag{4}$$

or

$$0.45 \leq We_s < 2.95 \qquad and \qquad 0.28\sqrt{1 - \frac{0.45}{We_s}} < I < \frac{\sqrt{0.53^2 + 8(0.53We_s)} - 0.53}{4.We_s} \tag{5}$$

where We_s, δ and I are respectively the symmetric Weber number, diameter ratio and impact parameter, given by:

$$We_s = We\frac{\delta^2}{12(1+\delta^3)(1+\delta^2)} \tag{6}$$

$$We = \rho_d d_s u_r^2/\sigma \tag{7}$$

$$\delta = d_s/d_l \tag{8}$$

$$I = 2b/(d_s + d_l) \tag{9}$$

where *We* is the Webber number considering ρ_d as the particle density, d_s the diameter of the smallest droplet (between the two droplets), u_r the relative velocity between the two particles and σ the surface tension; small and large droplet diameter d_s and d_l; b is the distance showed in Figure 3 and α is the collision angle.

Figure 3. Binary collision scheme, adapted from Huang and HanLiang (2013)

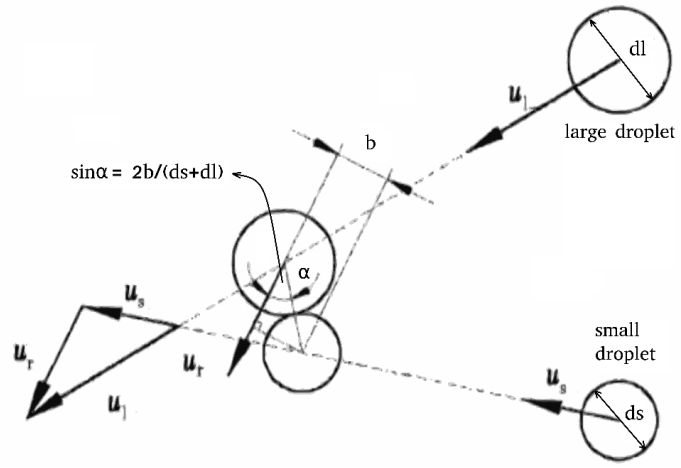

The instrumented workbench used in this work are sketched in Figure 4. It contains two modules, one (left hand) contains a liquid propellant tank, inert gas cylinder, control valves, pressure data acquisition system besides a set-up of light, lens and a FASTEC TS3100SC4 high speed camera. On the right hand of Figure 4 is the second module, it can be connected to the the first module in order to have their lines pressurize with fluids. A Spraytec laser diffraction system, valves and pressure transducers composes this module. Measurements with Spraytec system were taken at 50 mm downstream the impingement point.

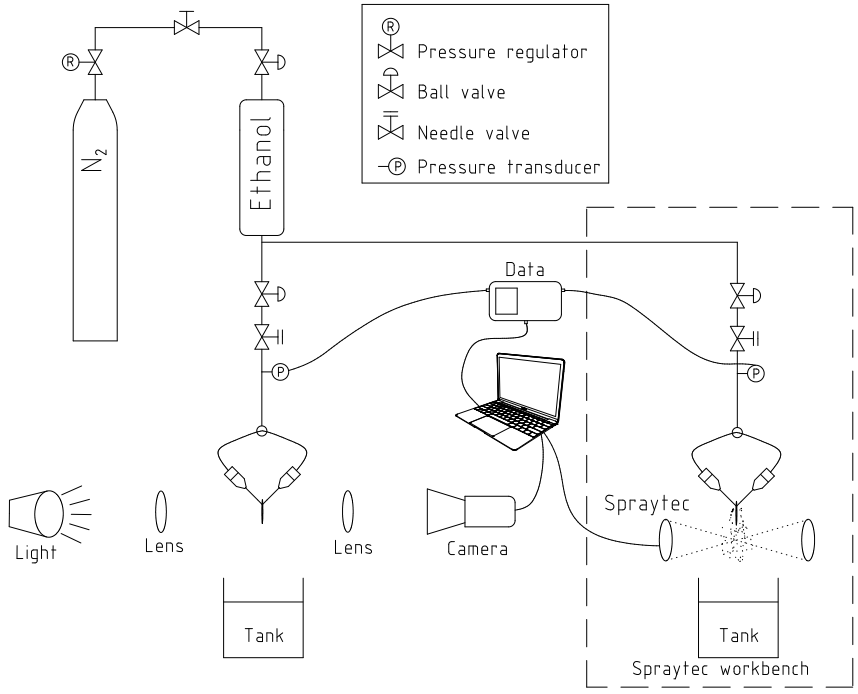

Figure 4. Experimental setup scheme.

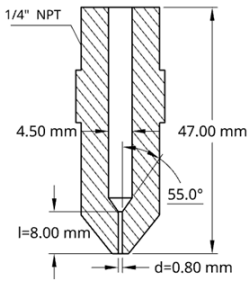

Figure 5. Injector. (Dias *et al.*, 2019b).

The inlet-chamfered jet injectors were made of Aluminium 6351 as depicted in Figure 5. It has orifice diameter (*D*) of 0.8 mm and orifice length (*l*) of 8.0 mm, resulting in a ratio *l/D=10*. The free jet length l_{pre} (or pre-impingement jet length) adopted was 6.0 mm, yielding a $l_{pre}/D = 7.5$ ratio (Dias *et al.*, 2019b).

Hydrous ethanol bought on Petrobras filling station was used, properties with references are shown in Table 1. The adopted refractive index for Spraytec measurements was 1.36.

Table 1. Hydrous ethanol properties with corresponding source.

Property	Value (Calculated[2] / Measured[3])
Concentration	[1] 93.8 $\sim$ 92.6 % (w/w)
Density at 20^{o}C	816.48 / 809.3 $[kg/m^3]$
Surface tension at 20^{o}C	21.10 / 23.00 $[mN/m]$
Viscosity at 20^{o}C	1.59 / 1.64 $[cP]$ or $[mPa.s]$

[1]considering min. and max. % (w/w), (Petrobras, 2019)
[2]calculated for 92.6 % (w/w) and T = 293.15 K (Khattab *et al.*, 2012)
[3](Fajgenbaum and Santos, 2013)

Hydrous ethanol was injected under a range of pressures while the exiting mass during 10 seconds were measured using a Shimadzu AUX 220 analytical balance. Figure 6 shows the corresponding mass flow rate and calculations for velocity, considering the orifice exit diameter and densities of fluids.

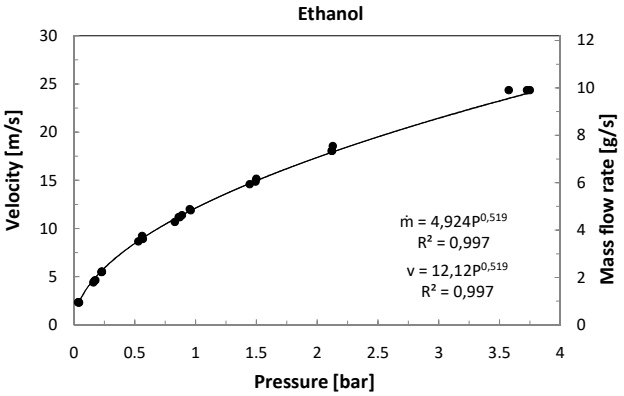

Figure 6. Velocity and mass flow rate for the designed injector

The performance of the two injectors proved to be practically identical in terms of discharge coefficient, leading to value of 0.75 when *Re*$\approx$ 11000 for liquids (Dias *et al.*, 2019a).

3. RESULTS

3.1 Free jet and sheet visualization

The internal injector geometry has a significant effect on jet flow, which can be in the laminar, transition or turbulent regimes before jet collision. In typical rocket engines, impinging jets of liquid propellants operate in turbulent flow Anderson *et al.* (2006). Pre-impingement jet behavior affects the formation of instabilities on the collision sheet and, consequently, influences spray formation.

Figure 7 shows shadow images of single round jets for hydrous ethanol obtained with the injector of Figure 5 for different injection pressures *P*, values of *We*, *Re* and *u* were calculated. Liquid jets of hydrous ethanol remain in the laminar regime only for small injection pressures and there is transition from laminar to turbulent regimes for most injection pressures. Plateau-Rayleigh instabilities are verified for *We* = 989.

Figure 8 shows the sheet evolution with increase of jet velocity. The sheet regimes goes from stable closed sheet (*u* = 2.81 m/s) to impact wave regime (*u* = 7.36 and 12.45 m/s). According to Dias *et al.* (2019b), stable closed rim for hydrous ethanol can be found until the Reynolds of jet reaches a value around 1700, considering the designed injector. Impact waves starts from the impingement point and grow in amplitude as the distance from the impingement point increase, as seen for *u* = 4.89 m/s. Transition regime can be verified when for *u* = 6.28 m/s.

Figure 7. Free jets in ambient air for increasing injection pressures.

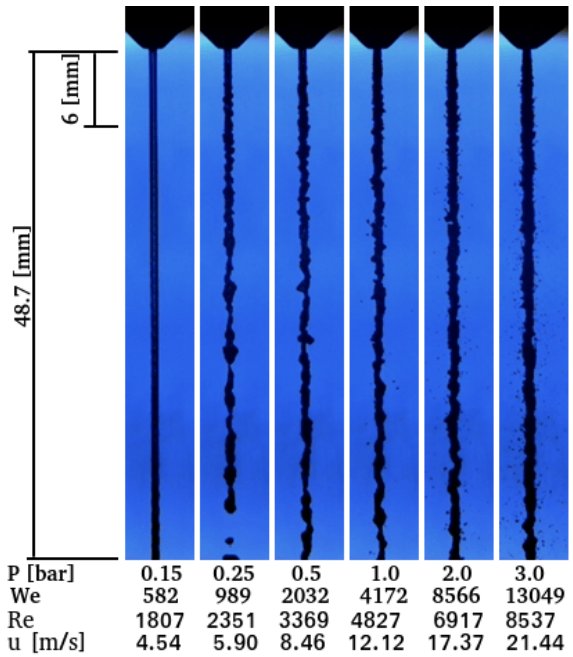

Figure 8. Hydrous ethanol sheet evolution with increasing of jet velocity, $2\theta = 75^o$.

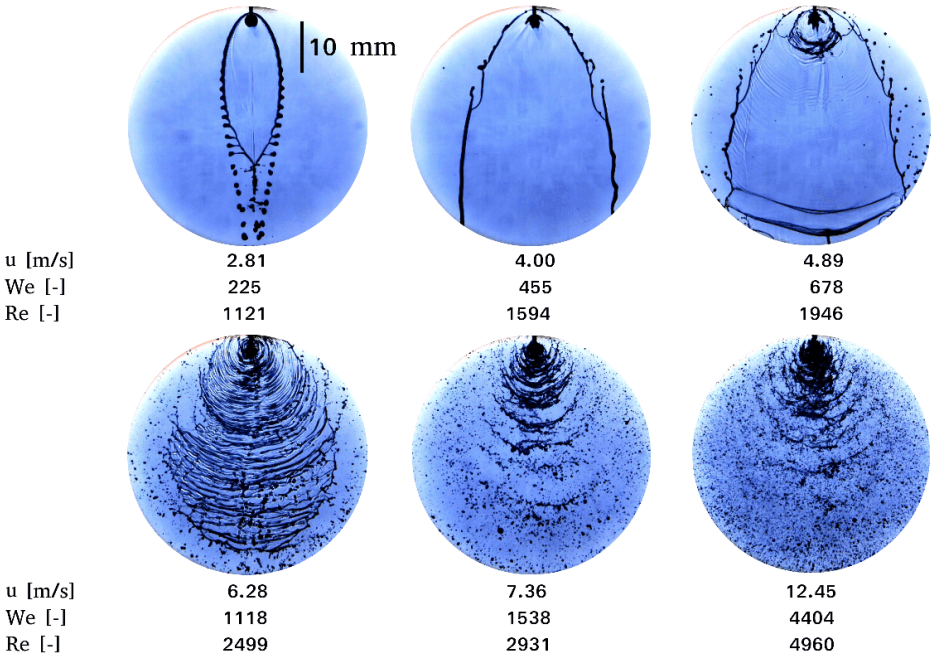

3.2 Coalescence and secondary breakup - brief analysis

Coalescence and secondary breakup may occur under specific conditions, as mentioned in the methodology section. The probability of encountering two particles was not calculated. However, when the ligaments are spread radially from the sheet formed on the impingement point, it is reasonable to estimate that the probability of a binary collision is low. On the other hand, the diffraction laser system determined volume concentrations from 124 to 184 ppm for hydrous ethanol

and from 73 to 80 ppm for water (in the same equipment and conditions, results for water are not reported in this work), with injection pressure of 1 bar and impingement angle of 75^o. Since the liquid hydrous ethanol spray is denser than the water spray, binary collisions in the hydrous ethanol spray are more probable than in the water spray.

Equations 4 to 9 were used to make a coalescence outcome analysis considering a possible binary collision on hydrous ethanol spray.

Table 2 shows coalescence analysis considering different relative jet velocities, diameters of large (dl) and small (ds) droplets and a fixed collision angle $\alpha = 30^o$.

Table 2. Coalescence analysis.

V. Relative [m/s]	dl=ds=100 um	dl=100, ds=50 um	dl=100, ds=25 um	dl=100, ds=12.5 um
11.25	-	-	-	coalesce
5.63	-	-	coalesce	coalesce
3.75	-	coalesce	coalesce	coalesce
2.81	-	coalesce	coalesce	coalesce
2.25	coalesce	coalesce	coalesce	coalesce
1.87	coalesce	coalesce	coalesce	coalesce

For secondary breakup analysis the particle Weber number considering the particle velocity equal to 80% of the jet velocity was used, which is a reasonable value due deceleration after the impingement. The lowest *We* value for droplet breakup is 12, corresponding to the called "bag breakup" Faeth *et al.* (1995). Table 3 shows the secondary atomization analysis, it brings jet velocities for the injection pressures used during atomization tests, particle velocities and particle diameters when *We* = 12, in other words, the minimum value of droplet diameter for bag breakup take place.

Table 3. Secondary atomization analysis.

P [bar]	Vjet [m/s]	Vpart = 0.8 Vjet	Diameter in μm when *We* = 12
1.0	12.12	9.70	2397
1.5	14.41	11.53	1695
2.0	17.37	13.90	1167
2.5	19.50	15.60	926
3.0	21.44	17.15	766
3.5	23.22	18.58	53

Particles with diameters between 0.1 to 2500 μm can be measured by Spraytec laser diffraction system, such range cover the diameters showed in Table 3. In the next results sections, experimental data of representative diameters and particle size distributions will be shown.

3.3 Representative diameters and particle size distributions

Sauter Mean Diameter *SMD* of hydrous ethanol is shown in Figure 9 for different *Re* or jet velocities and three different impingement angles (2θ). Plots indicate no regular trend of increase or decrease of *SMD*. The standard deviations of representative diameters of liquid ethanol are significantly large.

Figure 9. Hydrous Ethanol SMD as function of *Re* for a range of 2θ.

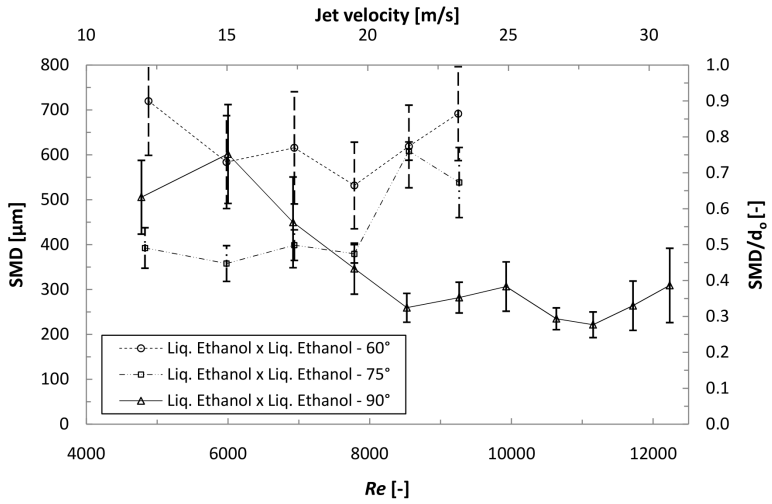

Figure 10 shows D_{v10} as function of *Re* for the values of 2θ range.

Figure 10. Hydrous Ethanol D_{v10} as function of *Re* for a range of 2θ.

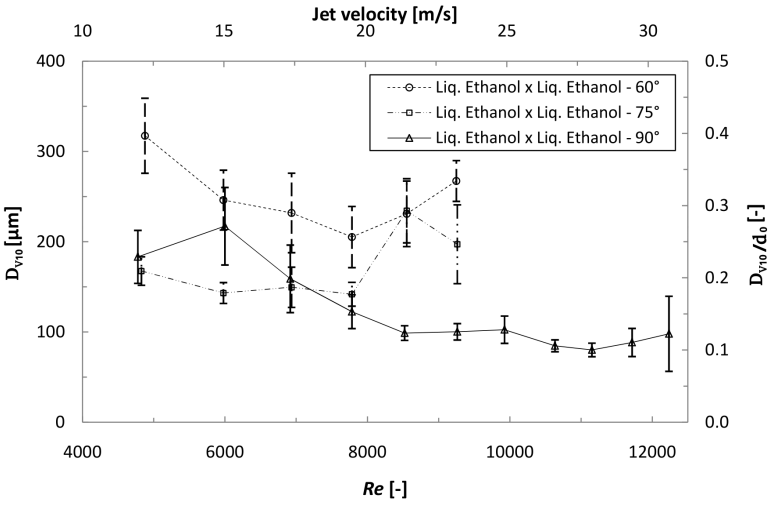

As verified for *SMD*, D_{v10} showed no clear trend in decrease the representative diameter as *Re* increased. However a trend in decrease of representative diameters with increase on 2θ seemed to happen. Such irregular behavior of representative diameter may encounter explanation on coalescence and secondary breakup atomization.

Cumulative volume as function of particle diameter graphs brings information about groups of particles that are more representative in terms of volume frequency, the analysis of such graphs is helpful to combustion applications.

Figure 11 shows particle size distribution graphs with increasing jet velocity. A detachment trend of the two droplet populations (bi-modal) with increasing jet velocity was verified. The absence of droplets of an intermediate size diameter may be an indication of secondary atomization, however the population of larger droplets tends to increase in volume frequency. Such intricate droplet size distribution may be a result of both secondary atomization for bag breakup and others modes (Figure 2) together with coalescence, the former being the major mechanism and later the minor. These mechanisms are probably the responsible for the large standard deviation on experiments *SMD*.

Droplet size measurements were also performed 80 mm downstream the impingement point and showed similar bi-modal behavior to measurements at 50 mm downstream the impingement point, indicating that the spray were already fully developed.

Sometimes the droplet size distributions can be multi-modal (Panão and Moreira, 2010)(Smyth and Hickey, 2003). According to Panão and Moreira (2010) multi or bi-modal drop size distributions do not refer to any measurement errors,

but come from the physical nature of the fragmentation process that have the simultaneous presences of primary, secondary or even tertiary droplets.

Figure 11. Droplet size distribution with increasing jet velocity - Ethanol.

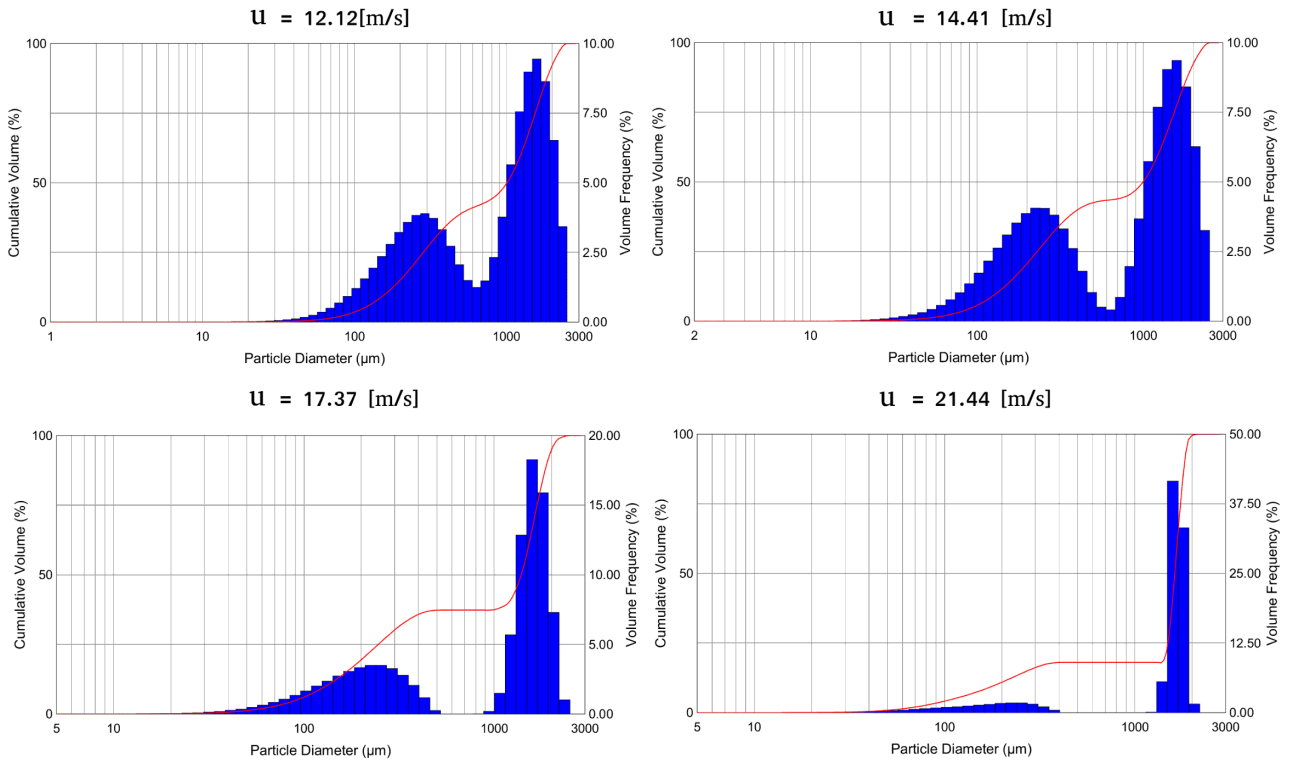

4. SUMMARY AND CONCLUSIONS

Impinging jets was widely used in rocket propulsion systems due its good atomization performance and simplicity. In this experimental work liquid hydrous ethanol was atomized using impinging jets. Tests for a range of injection pressures and impingement angles were performed. Shadow pictures of free jets in ambient air were taken for increasing pressure injections, the jet flow 6 mm downstream the exit was turbulent for velocities greater than approximately 5.0 m/s. The formed hydrous ethanol sheet was visualized for a range of *Re*, *We* and jet velocity, the identified regimes was from closed stable sheet to impact wave. A brief analysis of coalescence and secondary breakup was done based on literature simplified models to gain insight about phenomena taking place in a hydrous ethanol spray. Representative diameters and particle size distributions were obtained with a Spraytec laser diffraction system. Representative diameters SMD and D_{v10} showed no clear trend with increase of jet Reynolds number, however SMD and D_{v10} seemed to decrease with increasing 2θ. Bimodal particle size distributions presented a detachment trend of the two droplet populations with increasing jet velocity, however the population of larger droplets tends to increase in volume frequency. Such intricate droplet size distribution may be a result of both secondary atomization together with coalescence.

5. ACKNOWLEDGEMENTS

The authors acknowledge FAPESP for support through process 2016/21957-0 and CAPES for the M.Sc. scholarship granted to the first author.

6. REFERENCES

Anderson, W., Ryan III, H. and Santoro, R., 2006. "Impact wave-based model of impinging jet atomization". *Atomization and Sprays*, Vol. 16, pp. 791–805.

Ashgriz, N., 2011. *Handbook of Atomization and Sprays*. Springer, New York.

Chen, X. and Yang, V., 2019. "Recent advances in physical understanding and quantitative prediction of impinging-jet dynamics and atomization". *Chinese Journal of Aeronautics*, Vol. 32, No. 1, pp. 45–57.

Connell, T., Risha, G., Yetter, R. and Natan, B., 2018. "Hypergolic ignition of hydrogen peroxide/gel fuel impinging jets". *Journal of Propulsion and Power*, Vol. 34, No. 1, pp. 182–188.

Deng, H., Feng, F. and Zhuo, C., 2018. "A simplified linear model and breakup characteristics of power-law sheet formed by a doublet impinging injector". *Proc. IMechE Part G: Journal Aerospace Engineering*, Vol. 232, pp. 1035–1046.

Dias, G.S., Andrade, J.C., Fischer, G.A.A. and Costa, F.S., 2019a. "Coeficientes de descarga de injetores de jato". In *10º Workshop em Engenharia e Tecnologia Espaciais*.

Dias, G.S., Andrade, J.C., Fischer, G.A.A. and Costa, F.S., 2019b. "Experimental study of atomization by impinging jets of liquid and gelled green propellants". In *25th International Congress of Mechanical Engineering (COBEM 2019)*. pp. 1–7.

Faeth, G.M., HSIANG, L. and Wu, P., 1995. "Structure and breakup properties of sprays". *Int. J. Multiphase Flow*, Vol. 21, pp. 99–127.

Fajgenbaum, R. and Santos, R.G., 2013. "Influence of ethanol temperature on atomization parameters from a multi-hole port fuel injector". In *22nd International Congress of Mechanical Engineering (COBEM 2013)*. pp. 3823–3830.

Fakhri, S., Lee, J.G. and Yetter, R.A., 2010. "Effect of nozzle geometry on the atomization and spray characteristics of gelled-propellant simultants formed by two impinging jets". *Atomization and Sprays*, Vol. 20, No. 12, pp. 1033–1046.

Ghafourian, A., Mahalingam, S., Dindi, H. and Daily, J.W., 1991. "A review of atomization in liquid rocket engines". 29th Aerospace Sciences Meeting, Reno, Nevada, US.

Huang, Z. and HanLiang, B., 2013. "Inumerical prediction of the outcomes of binary-droplet collision in steam-water separator". In *21st International Conference on Nuclear Engineering*. pp. 1–5.

Khattab, I., Bandarkar, F., Abolghassemi Fakhree, M.A. and Jouyban, A., 2012. "Density, viscosity, and surface tension of water+ ethanol mixtures from 293 to 323k". *Korean Journal of Chemical Engineering*, Vol. 29, pp. 812–817.

Khavkin, Y.I., 2004. *Theory and practice swirl atomizers*. Taylor & Francis, New York, 1st edition.

Lefebvre, A., 1988. *Atomization and Sprays*. Taylor Francis, West Lafayette, Indiana.

Negri, M. and Ciezki, H.K., 2016. "Atomization of viscoelastic fluids with an impinging jet injector: morphology and physical mechanism of thread formation". *Atomization and Sprays*, Vol. 27, pp. 319–336.

Panão, M. and Moreira, A., 2010. "Physical analysis of multimodality in atomization processes". In *23rd Annual Conference on Liquid Atomization and Spray Systems*. pp. 1–11.

Petrobras, 2019. "Ficha de informações de segurança de produto químico -fispq". *https://www.br.com.br/ - Access Date: 03/03/2020*.

Rabe, C., Malet, J. and Feuillebois, F., 2010. "Experimental investigation of water droplet binary collisions and description of outcomes with a symmetric weber number". *Physics of Fluids*, Vol. 22, No. 4, p. 047101.

Ramasubramanian, C., Notaro, V. and Lee, J.G., 2015. "Characterization of near-field spray of nongelled- and gelled-impinging doublets at high pressure". *Journal of Propulsion and Power*, pp. 1–11.

Smyth, H. and Hickey, A., 2003. "Multimodal particle size distributions emitted from hfa-134a solution pressurized metered-dose inhalers". *AAPS PharmSciTech*, Vol. 4, No. 3, p. 1–11.

7. RESPONSIBILITY NOTICE

The authors are the only responsible for the printed material included in this paper.